Effects of Heating Rate During ACFs Curing Process on Material Properties andThermal Cycling Reliability of Flip Chip Assembly

Kyung-Woon Jang and Kyung-Wook Paik
Dept. of Materials Science and Engineering
Korea Advanced Institute of Science and Technology
373-1 Guseong-dong, Yuseong-gu, Daejeon 305-701, Republic of Korea
e-mail : amiha@kaist.ac.kr, phone : +82-42-869-3375, Fax : +82-42-869-3310

Abstract

In this study, effects of heating rate during ACF curing processes on material properties such as thermo-mechanical properties and rheological properties of ACFs were investigated. Generally, material properties of polymers change with the process conditions such as temperature, time, frequency, and so on. As the heating rate increased, coefficient of thermal expansion (CTE) of ACFs increased, and storage modulus and glass transition temperature (T_g) of ACFs decreased. ACF material property changes were due to cross-linking density which is related with ACFs density.

Contact resistance of ACFs flip chip assembly was dependent on heating rates. As the heating rate increased, the contact resistances of ACFs flip chip assemblies decreased. The decrease in contact resistance was due to larger ACFs conductive particle deformation. In addition, effects of heating rates of ACFs on thermal cycling (T/C) reliability of flip chip assemblies were also investigated. As the heating rate increased, the contact resistances of ACF flip chip assemblies rapidly increased during the T/C test. T/C reliability test result was analyzed by the shear strain estimation which is closely related with ACFs material properties and the gap between a chip bump and a substrate pad.

As a summary, effects of heating rate on ACFs material properties and thermal cycling reliability were investigated. T/C reliability test result was analyzed in terms of the shear strain. Based on the results, the guidelines of ACFs curing process during flip chip bonding processes were suggested.

1. Introduction

In flip chip technology, epoxy based materials such as ACFs and underfills not only redistribute the stress and strain caused by CTE mismatch between a chip and a substrate but also hold the flip chip joint from mechanical deformation. [1]-[2] These epoxy based materials have been used to improve the fatigue life or T/C reliability of flip chip assemblies. Among the epoxy based materials, the usage of ACFs has been increasing in many areas such as Chip-on-Glass (COG), Chip-on-Flex (COF), Chip-on-Board (COB), and Flex-on-Board (FOB) because of low temperature processing (150 ºC to 180 ºC), fine pitch interconnection (below 50 μm), low cost capability (no flux and underfilling), and green process (no lead and solvents). As the usage of ACFs is increasing, reliability of ACFs flip chip assemblies has been widely studied to apply ACFs for various flip chip applications. It has been widely known that thermo-mechanical reliability of flip chip assembly is dominated by thermo-mechanical properties of ACFs such as coefficient of thermal expansion (CTE),

storage modulus, and glass transition temperature (T_g). In addition, ACFs material properties are affected by environmental conditions such as temperature, time, and humidity, because ACFs are polymer materials. [3] However, effects of flip chip bonding conditions such as curing temperatures and heating rates on ACFs material properties and ACFs flip chip reliability have not been reported.

When ACFs are cured from a B-stage state to a cured solid state, there are chemical and thermal shrinkages induced. And finally, thermo-mechanical properties of ACFs are established by the curing process. As previously mentioned, it can be easily expected that thermo-mechanical properties of ACFs are dependent on the curing process conditions such as curing temperatures and heating rates. In addition, the thermo-mechanical properties of ACFs determine the ACFs flip chip assembly reliability. In other words, ACFs curing process conditions can affect both ACFs flip chip assembly reliability and the productivity of ACFs flip chip assemblies. In two viewpoints of productivity and reliability, ACFs curing conditions should be optimized. In this study, the heating rate of the curing process was focused to investigate the ACFs material property changes such as CTE, modulus, T_g, density, and temperature related viscosity. In addition, the relationship between heating rates of ACFs and flip chip assembly performances was also investigated in terms of contact resistance and T/C reliability of ACFs flip chip assemblies. Finally, the guideline of optimum heating rate of ACFs during curing processes was suggested for high performance of ACF flip chip assembly.

2. Experimental

2.1. ACFs material

ACFs material used in this study is basically composed of bisphenol-A liquid epoxy, conductive particle, silica filler, curing agent and so on. The total thickness of ACF was 50 μm, which consists of 30 μm NCF layer and 20 μm ACF layer. For the thermo-mechanical property measurements, ACFs were cured with various heating rates of 1, 5, 10, and 20 ºC/sec from room temperature to 190 ºC and also isothermally cured at 190 ºC on a heating rate controllable hot-plate. Isothermal cure indicates that ACF is abruptly placed on 190ºC hot-plate manually. It is assumed that isothermal cure has almost infinite heating rate.

2.2. TMA and DMA analysis

To investigate thermo-mechanical properties of cured ACFs with various heating rates, TMA and DMA analysis were performed. In TMA analysis, coefficients of thermal expansion (CTE) of ACFs were measured. Specimens which have dimension of 1.5~2 mm width and 100~150 μm

thickness were subjected to 100 mN uniaxial tensile load from 30 °C to 200 °C with 5 °C/min heating rate. The CTE values were calculated from the linear section of dimensional changes versus temperatures.

In DMA analysis, the storage modulus and loss tangent (tan δ) were measured using the same samples as TMA analysis. Specimens were under sinusoidal force of 200 mN ± 100 mN at 0.02 Hz. The temperature range and heating rate were the same as in TMA analysis. The changes in specimen length were recorded with the cyclic force. The data were then processed to determine the visco-elastic properties.

2.3. ACFs viscosity

B-stage ACF viscosity according to the heating rate was measured using a rotational rheometer. 1 mm thick ACFs were prepared by laminating many ACF layers. The samples were heated from 40 ºC to 200 ºC at 1, 3, 5, 10 and 30 ºC/min of heating rates. Shear stress of 1000 Pa was applied to the samples at 1 Hz frequency at constant stress mode. Figure 1 shows photo image of the set-up for ACFs viscosity measurement.
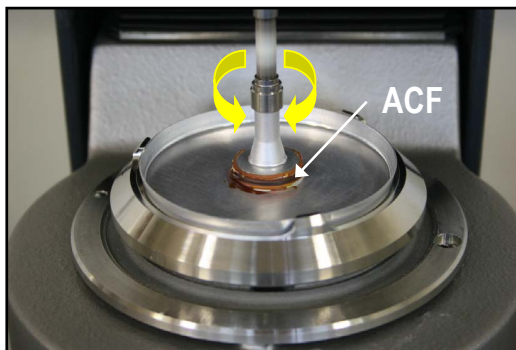

Figure 1. Photo image of the set-up for ACFs viscosity measurement.

2.4. ACFs density

In order to investigate the ACFs material property changes, ACF densities according to heating rates were measured by the Archimedes method. For the precise measurement, larger mass and volume of test samples were prepared by laminating several ACF layers.

2.5. Contact resistance

Figure 2 shows photo image of the fabricated ACFs flip chip assembly sample for in-situ contact resistance measurement. For the measurement, 8 mm × 8 mm × 670 μm chip and 1 mm thick substrate were used. The experimental procedures are as follows. At first, metal wires were attached to Cu probing pads by Pb welding. Secondly, a thermocouple was put on the substrate and then ACF was pre-laminated above. Finally, changes in both in-situ contact resistance and ACF temperature were measured at the same time using a LCR meter and a thermometer during flip chip assembly process. The applied force was 50 N, and the maximum temperature was 190 ºC for flip chip bonding process. During the flip chip bonding process, the in-situ contact resistance of a single ACF joint was measured by using the four point probe method shown in Figure 3. In addition, the gaps

between chip bumps and substrate pads of ACF flip chip assembly joints according to heating rates were observed in SEM images to investigate the differences in contact resistances.
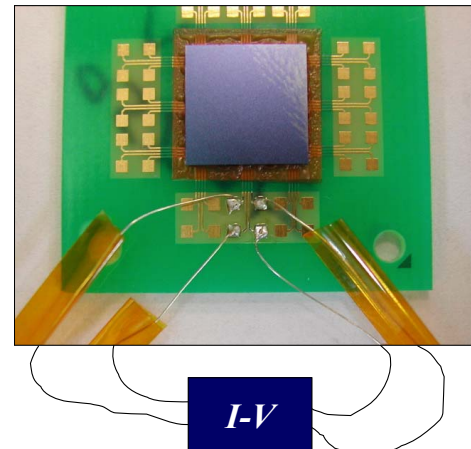

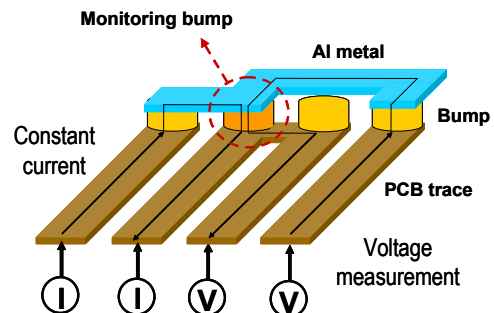Figure 2. Photo image of ACFs flip chip assembly sample for in-situ contact resistance measurement.

Figure 3. Four-point probing structure of a single ACF joint for contact resistance measurement.

2.6. T/C reliability test

To investigate effects of heating rates on ACFs flip chip assembly reliability, contact resistances of ACFs flip chip assemblies cured with various heating rates were monitored during T/C test. The T/C test profile was 150 ºC (15 min) and -40 ºC (15 min). The number of samples of each condition was 5 and each ACF flip chip assembly has 12 four-point probing structures for contact resistance measurement.

3. Results and Discussion

3.1. TMA and DMA analysis

Figure 4 shows dimensional changes of ACFs according to various heating rates. As shown in Figure 4, as the heating rate increased, the CTE of ACF gradually increased. Also, the second region which dimensional change abruptly increases was observed presumably due to an excess free volume. [4] From the result, it is considered that ACFs heating rate may affect the excess free volume and cross-linking density. The relationship between ACFs heating rates and cross-linking density will be discussed afterwards.
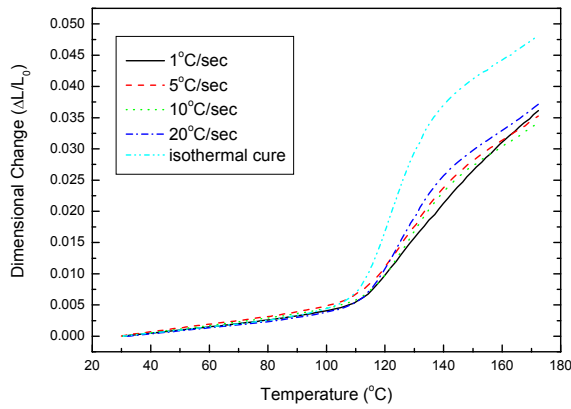
Figure 4. Dimensional changes of ACFs according to heating rates.

Figure 5 shows modulus and loss tangent changes of ACFs according to heating rates. As the heating rate increased, both modulus and T_g, which is considered as a peak temperature of loss tangent, decreased. The measured thermo-mechanical properties of ACFs with various heating rates were listed in Table 1.

It is understood that thermo-mechanical properties of ACFs are dependent on curing conditions such as curing temperature, heating rates and times. Also, ACFs thermo-mechanical property changes are presumably due to free volume or induced stress and strain caused by the curing shrinkage during curing processes.

Table 1. ACFs thermo-mechanical properties according to heating rates.

Heating rates	CTE below T_g ($\alpha1$)	CTE above T_g ($\alpha2$)	Modulus at 30 ºC	T_g
1 ºC/sec	38.9	553	3.1 GPa	112.5
5 ºC/sec	46.4	840	3.1 GPa	108.7
10 ºC/sec	45.6	736	3.0 GPa	108.6
20 ºC/sec	50.6	895	2.5 GPa	108.5
Iso. cure	59.2	1392	2.2 GPa	104.4

3.2. ACFs viscosity

Figure 6 shows ACF viscosity changes according to heating rates. ACF experiences the first 'flow' region where the viscosity decreases as the temperature goes up. And then, as ACF curing reaction goes on, ACF viscosity increases within the second 'gelation' region. Finally, ACF has stable high viscosity after curing reaction completed. As you can see in Figure 6, as the heating rate increased, the curing onset temperature shifted to higher temperatures, and the minimum viscosity of the curves gradually decreased. It may be considered that chain mobility can't follow up the curing reaction rate resulting in an increased curing onset temperature. This result will be discussed with next contact resistance result afterwards.
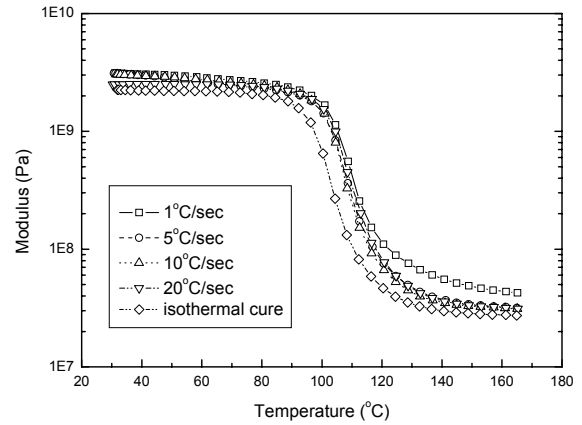
(a)
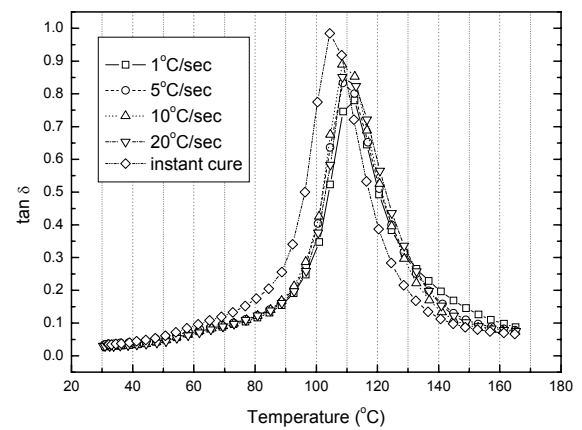
(b)

Figure 5. (a) Modulus changes and (b) loss tangent changes of ACFs according to heating rates.
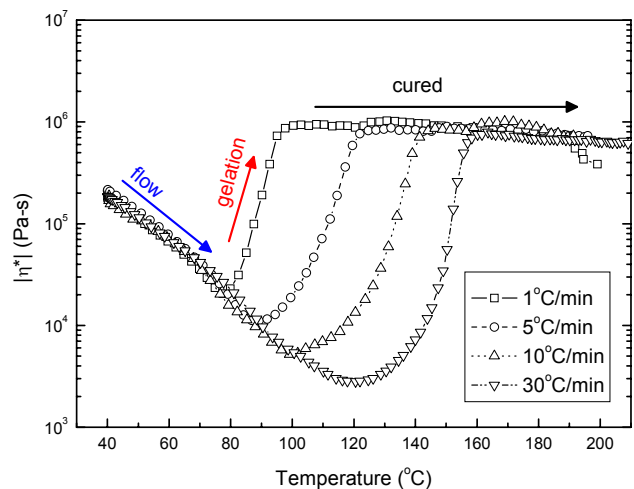

Figure 6. ACF viscosity changes according to heating rates.

3.3. ACFs density

Figure 7 shows ACF density changes according to heating rates. As the heating rate increased, ACF density gradually decreased. Low density means that many micro-voids which are related with excess free volume exists inside cured ACFs resulting in lower ACFs cross-linking density. ACF polymer molecular chains may have enough time to freely move and form long molecular chain structures, as the heating rate decreases. In order to calculate ACFs cross-linking densities according to heating rates, Nielsen's equation was used. [5]-[6]

$$\nu = \frac{Er}{3RT} \qquad (1)$$

Where ν represents the cross-linking density (number of moles of chains per cm^3), R is the gas constant (8.314 J/K·mole), T is the temperature in Kelvin at 40ºC above the glass transition temperature of the samples, and Er is the elastic modulus. Calculated ACFs cross-linking densities using the equation (1) are listed in Table 2. As expected, as the heating rate increased, ACF cross-linking density decreased.

Table 2. ACF cross-linking densities according to heating rates.

Heating rates	1 ºC/sec	5 ºC/sec	10 ºC/sec	20 ºC/sec	Iso.
Modulus at T_g + 40ºC (MPa)	46.5	34.0	33.3	33.0	32.6
T_g	112.5	108.7	108.6	108.5	104.4
Cross-linking density (10^{-3}moles/cm³)	4.38	3.23	3.17	3.14	3.13

3.4. Contact resistances

Figure 8(a) and (b) show in-situ contact resistance changes of ACFs flip chip assemblies as a function of times and temperatures according to heating rates. Figure 9 shows contact resistances of ACF flip chip assemblies at room temperature according to heating rates. As the heating rate increased, electrical contact build-up temperature shifted to higher temperatures, and the contact resistance at room temperature decreased. Figure 10 shows SEM images of ACF joints of the flip chip assemblies according to heating rates. In SEM images, as the heating rate increased, the ACF joint gap between a chip bump and a substrate pad gradually decreased and the amount of conductive particle deformation increased. As the amount of conductive particle deformation increases, contact resistance decreases because of increase in contact area between chip bump and metal layer of conductive particle. The SEM images support the contact resistance results and this result represents the ACF viscosity changes. In other words, ACFs can easily flow at reduced ACF viscosity and conductive particle can be easily deformed at the same force.
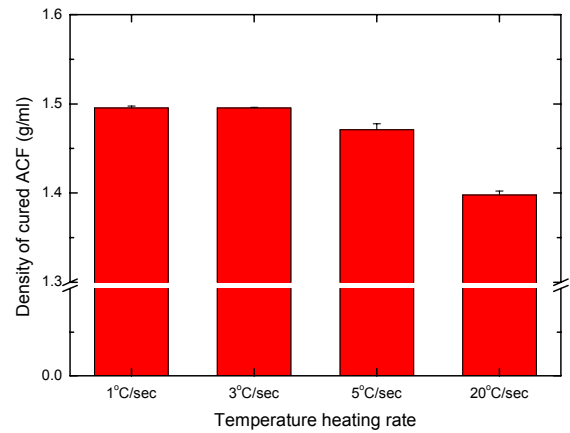

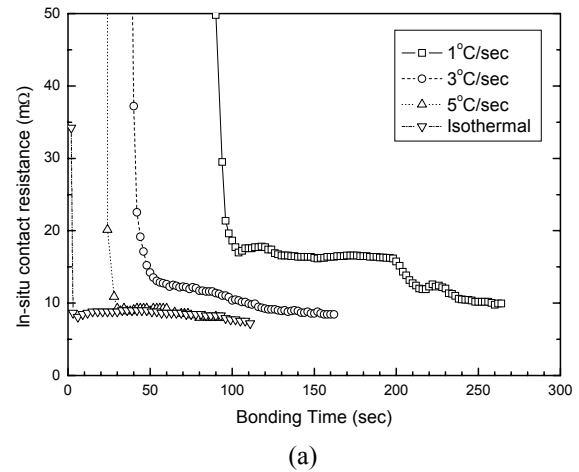Figure 7. ACF density changes according to heating rates.

(a)

Figure 8 (a). In-situ contact resistance changes according to heating rates as a function of time.
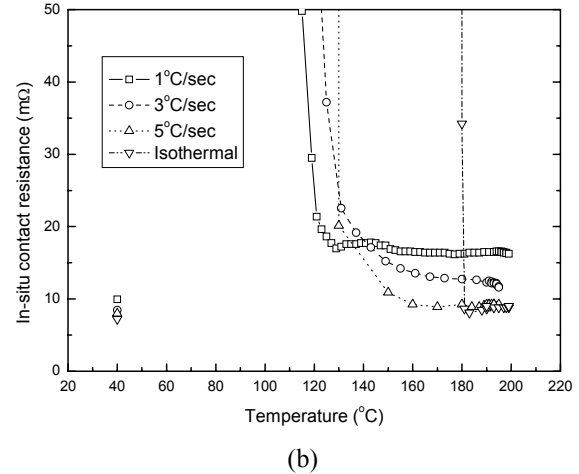

(b)

Figure 8 (b). In-situ contact resistance changes according to heating rates as a function of temperature.
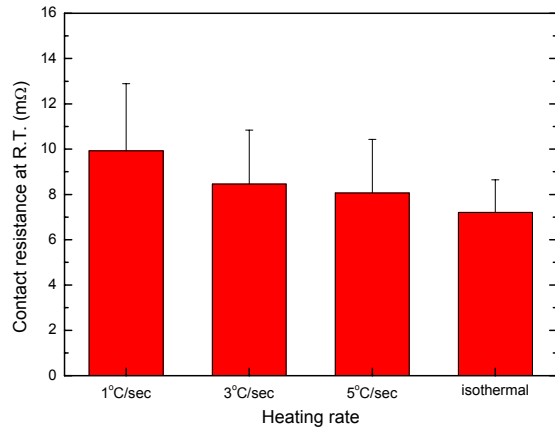
Figure 9. Contact resistances of ACFs flip chip assemblies at room temperature.

(a) 1℃/sec   (b) 3℃/sec
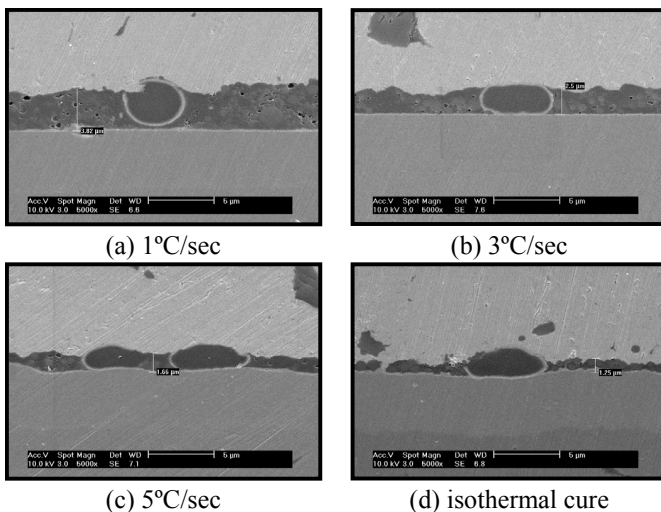
(c) 5℃/sec   (d) isothermal cure

Figure 10. SEM images of ACF flip chip assembly joints according to heating rates.

Based on the results, ACF joint formation processes are as follows. At first, as the temperature goes up, ACF resin flows and spreads out from the gap between a chip bump and a substrate pad due to reduced ACF viscosity. Secondly, conductive particles are trapped in the gap between a chip bump and a substrate pad. As the temperature goes up more and more, ACF resin cured and ACF joints have electrical contact after curing processes completed. This explanation is strongly supported by ACF viscosity changes and contact resistance changes of ACFs flip chip assemblies.

3.5. T/C reliability

Figure 11 shows cumulative distributions of contact resistance changes of ACFs flip chip assemblies according to heating rates during T/C test. As can be seen in Figure 11, contact resistances of flip chip assembly had higher heating rates rapidly increased. In case of 1 ℃/sec, the contact resistances of flip chip assemblies were stable after 729 cycles. On the other hand, in case of the isothermal cure, open

failure which means contact resistance cannot be measured showed up just after 200 cycles. As expected from previous results, ACFs flip chip assembly which had lower heating rates showed better T/C reliability. It is widely known that higher CTE and lower modulus ACFs result in a larger shear strain. Therefore, it is clear that deteriorated ACFs material properties with higher heating rates enlarge shear strain at the flip chip joint. In addition, the reduced gap between a chip bump and a substrate pad induced by increased heating rates also related with larger shear strain. When an electronic package device in under thermal loading, thermally-induced stresses and strains are generated by CTE mismatch among different materials, thermal gradients, and geometric constraints. While the temperature increases from lower temperature to higher temperature, the difference in CTE between a chip and a substrate causes shearing in the ACF joints. When the temperature goes up from T_L to T_H, the shear strain caused by a thermal loading is defined as :

$$\gamma = \frac{L}{h}(\alpha_b - \alpha_c)(T_H - T_L) \qquad (2)$$

where L is the distance of the ACF joint from the neutral point, h is the gap distance of the ACF joint, α_b is the CTE of a board, and α_c is the CTE of a chip. [7]

From the equation (2), as the gap distance of ACFs joint increases, shear strain caused by thermal loading decreases. Therefore, small gap between a chip bump and a substrate pad induced by an increased heating rate can also increase the shear strain.

Conclusions

In this study, the effects of heating rate on material properties of ACFs were investigated. Also, contact resistance changes were measured. In a viewpoint of ACF thermo-mechanical properties, as the heating rate increased, CTE increased, and both modulus and T_g decreased. Moreover, ACF curing onset temperature shifted to higher temperatures and the minimum viscosity decreased as increased heating rates. These results were closely related with contact resistance changes of ACFs flip chip assemblies. In addition, as the heating rate increased, ACF density decreased. ACF polymer chains cannot have enough time to freely move so polymer chain mobility cannot follow up the curing reaction rate. It was also supported by calculated ACF cross-linking density changes.

As the heating rate increased, contact resistance decreased. The electrical contact build-up temperature shifted higher temperatures. Also, the gap between a chip bump and a substrate pad gradually decreased, because the amount of conductive particle deformation increased in SEM images. It is because conductive particles can be easily deformed by a reduced ACF viscosity. In T/C test, as the heating rates decreased, ACF flip chip assemblies showed better T/C reliability in terms of contact resistance. Enhanced ACFs material properties established with lower heating rates decreased the shear strain of ACFs flip chip joint. A larger gap between a chip bump and a substrate pad induced by lower heating rates may also decrease the shear strain.

Conclusively, ACFs material properties such as CTE, modulus, and T_g closely related with a cross-linking density depended on the heating rates. The larger shear strain induced by higher heating rates deteriorated ACF flip chip reliability easily. Higher heating rates are preferred in a viewpoint of mass production, but deteriorate ACF material properties and ACF flip chip reliability. Therefore, the optimum heating rates should be determined for ACF flip chip applications.

References

1. Liu, J., "An overview of Advanced of Conductive Adhesive Joining Technology in Electronics Applications," *Materials Technology*, Vol. 10 (1998), pp.247-252.

2. Yim, M.-J., "A study on the Electrical Conduction Mechanism of Anisotropically Conductive Film for LCD Packaging Application," *Proc 1997 ASME international and intersociety Electronic/Photonic Packing Conf.*, Kohala Coast, Hawaii, June. 1997, pp. 65-72.

3. Krevelen, D. W., Properties of Polymers, Elsevier (Amstredam, 1997).

4. Li, S., "Studies on Relaxation and Thermal Expansion Behavior of Polysiloxane-Modified Epoxy Resin," *Journal of Macromolecular Science. Part B : Physics*. Vol. 36, No. 3 (1997), pp. 357-366.

5. Shan, L., "Effect of network structure of epoxy DGEBA-poly(oxypropylene)diamines on tensile behavior," *Journal of Polymer Science. Part B : Polymer Physics*, Vol. 37 (1999), pp. 2185-2819.

6. Nielsen, L. E., "Cross-linking—effect on physical properties of polymers," *Journal of Macromolecular Science Chemistry*, Vol. C3 (1969), pp. 69.

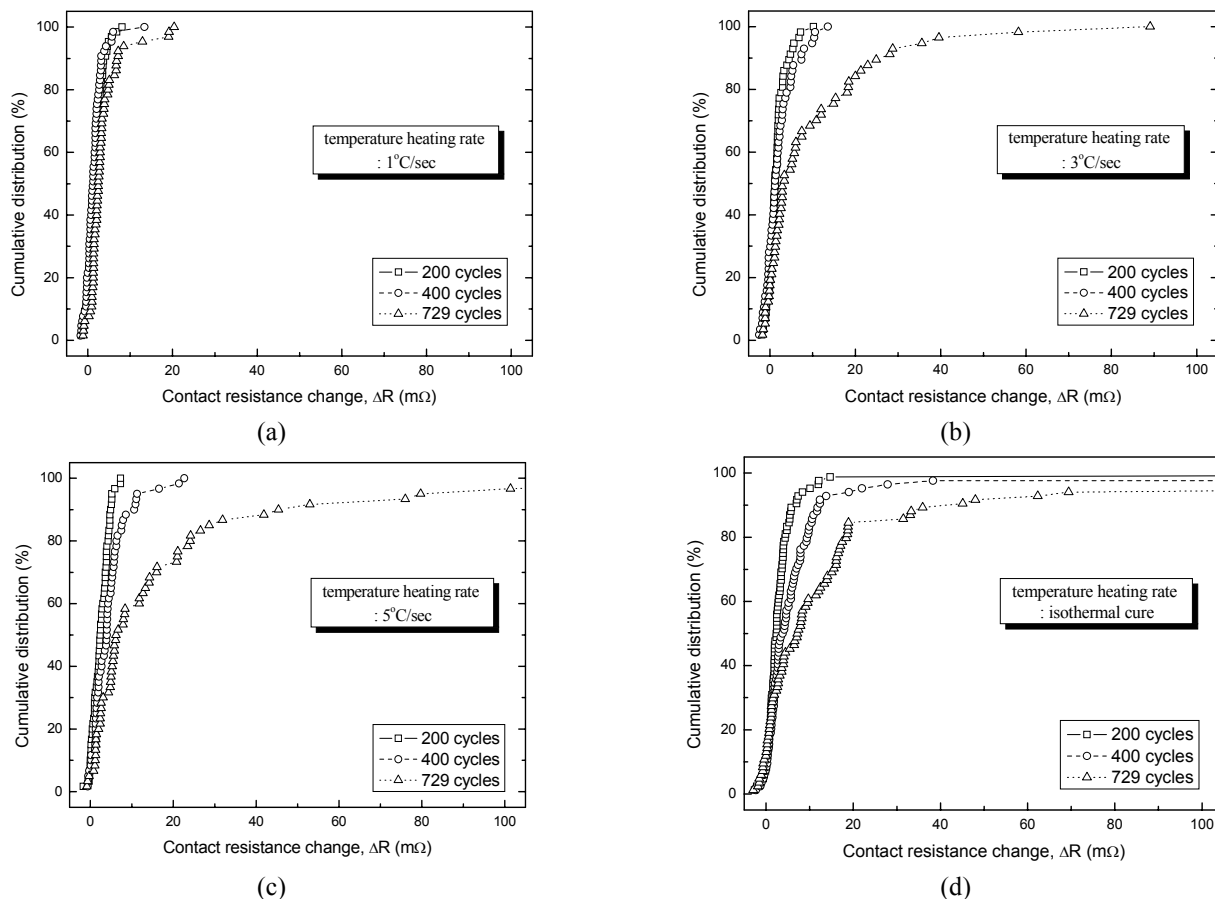7. Tummala, Rao R., Fundamentals of Microsystems Packaging, McGraw-Hill (New York, 2001), pp. 188-189.

Figure 11. Cumulative distributions of contact resistance changes according to heating rates during T/C test.